J Mater Sci (2010) 45:3671–3676
DOI 10.1007/s10853-010-4412-9

Preparation and properties of pressureless-sintered porous Si_3N_4

Hongjie Wang · Juanli Yu · Jian Zhang · Dahai Zhang

Received: 7 December 2009 / Accepted: 11 March 2010 / Published online: 30 March 2010

Abstract Wave-transparent materials used at high temperature environment generated by high supersonic and hypersonic speeds must possess excellent mechanical property. In this paper, porous Si_3N_4 ceramics with high strength were fabricated by low molding pressure (10 MPa) and pressureless sintering process, without any other pore forming agents. The sintering behavior and the effect of porosity on the mechanical strength and dielectric properties were investigated. The flexural strength of porous Si_3N_4 ceramics was up to 57–176 MPa with porosity of 45–60%, dielectric constant of 2.35–3.39, and dielectric loss of 1.6–3.5 $\times$ 10^{-3} in the frequency range of 8–18 GHz, at room temperature. With the increase of porosity, the flexural strength, dielectric constant, and dielectric loss all decreased.

Introduction

Broadband radomes in the high temperature environment generated by high supersonic and hypersonic speeds must possess structural adequacy to withstand severe thermal and aerodynamic loads as well as erosion effects due to rain and dust [1], such as the low dielectric constant, high mechanical strength, excellent thermal shock resistance, and rain erosion resistance, etc.

In the past years, polytetrafluoroethylene, Al_2O_3, SiO_2, and its composites were all used as radome materials. The applied temperature of polytetrafluoroethylene is lower than 500 °C because of its chemical bonding. Al_2O_3 has rather high strength, high hardness, and good rain erosion resistance. However, Al_2O_3 has relative high dielectric constant, and the dielectric constant increases with the increase of temperature. In the meantime, Al_2O_3 has poor thermal shock resistance. Fused silica (SiO_2) was used for radome materials owing to its rather low dielectric constant and loss tangent, high chemical stability, high melting point, and extremely low coefficient of thermal expansion [2, 3]. However, it has poor strength (about 50 MPa) and poor rain erosion resistance.

Silicon nitride (Si_3N_4) ceramics have excellent mechanical properties (such as high strength, high fracture toughness at both room and elevated temperatures, high thermal shock resistance, and high chemical resistance) [4, 5], and thus it has great promise for high temperature applications. However, Si_3N_4 ceramics have moderate dielectric constant (5.6–5.8 for reactive sintered Si_3N_4 and 7.9–8.2 for hot-pressed Si_3N_4 at 8–10 GHz) [6–8], which makes Si_3N_4 inadequately used for radome materials. At present, porous Si_3N_4 ceramics with high mechanical strength and low dielectric constant were emphasized.

As we all know, the dielectric constant of air is nearly 1, and its loss tangent is about 0. The introduction of pores gives rise to an effectively reduced dielectric constant, and this lowering is particularly remarkable when the porosity is enhanced to 35% or above. For example, a porous Si_3N_4 ceramic with a porosity of 40–55% attained a low-dielectric constant of 2.7–3.3 [9, 10]. In the meantime, the thermal conductivity can also be lowered because of the existence of

H. Wang (✉) · J. Yu
State Key Laboratory for Mechanical Behavior of Materials, School of Materials Science and Engineering, Xi'an Jiaotong University, 28 Xian Ning Road, Xi'an 710049, People's Republic of China
e-mail: hjwang@mail.xjtu.edu.cn

J. Zhang · D. Zhang
National Key Laboratory of Advanced Functional Composite Materials, Beijing 100076, China

pores. Therefore, porous ceramics can be generally believed as promising radome materials. But pores in ceramics can also be considered as the crack, which will deteriorate the mechanical properties of materials.

Porous Si_3N_4 ceramics can be prepared by many approaches including adding pore forming agents [11], foaming [12], the polymeric sponge impregnation [13], freeze drying [14], carbothermal nitridation [15, 16], gel casting [17, 18], etc. Recently, porous Si_3N_4 ceramics have been fabricated via low temperature sintering, using H_3PO_4 and H_3BO_3 as pore forming agent, which had a high strength of 130 MPa with a dielectric constant of 4.6 in the frequency range of 100 MHz to 1 GHz at room temperature [19]. Li [10] fabricated a porous Si_3N_4–SiO_2 composite using phenolic resin as pore forming agent, which had a flexural strength of 120 MPa, and a dielectric constant of 3.8 with a dielectric loss of 3.11×10^{-3} at a resonant frequency of 14 GHz [20].

In this work, porous Si_3N_4 ceramics with the flexural strength of 57–176 MPa, the porosity of 45–60%, and the dielectric constant of 2.35–3.39 were prepared from α-Si_3N_4 powder, using Y_2O_3 and Al_2O_3 as the sintering aids, at 1600–1800 °C in N_2 atmosphere by low molding pressure (10 MPa) and pressureless sintering. The sintering behavior of porous Si_3N_4 ceramics and the effect of porosity on the flexural strength and dielectric constant were investigated.

Experimental procedure

Preparation of porous samples

Si_3N_4 powders (mean particle size: 0.37 μm, α phase >94 wt%, Si < 0.5%) were employed in this study and supplied by Shanghai Junyu Ceramics Co. Ltd., Shanghai, China. Al_2O_3 powders (mean particle size: 1.07 μm, 99% purity, Shanghai Junyu Ceramics Co. Ltd., Shanghai, China) Y_2O_3 (mean particle size: 4.74 μm, 99.9% purity, Shanghai Yuelong New Materials Co. Ltd., Shanghai, China) were used as the sintering additives. The content of Y_2O_3 was 5 wt% and Al_2O_3 was 3 wt% based on the Si_3N_4 powders, respectively.

The powders were ball-milled in ethanol for 24 h using an agent media to obtain homogeneous slurry. The slurry was dried and sifted out by crushing with a 200 mesh sieve, and then the resultant powder mixture was cold-pressed under 10 MPa using a round steel die. The specimens with a dimension of $\phi 60 \times 5$ mm were pressureless- sintered at 1600–1800 °C holding for 30–120 min in a N_2 atmosphere (0.225 MPa), and subsequently allowed to cool naturally. In the experiment, the N_2 atmosphere (0.225 MPa) was used only as protecting atmosphere to avoid the volatilization of Si_3N_4 at high temperature.

Characteristic and test

The porosity of the sintered sample was measured by the Archimedes displacement technique. The bulk density (ρ_0) and the true density (ρ) of the sintered body were determined by Archimedes' method in water and by water displacement method, respectively. Then the porosity (P) was calculated as follows:

$$P = \left(1 - \frac{\rho_0}{\rho}\right) \times 100\% \quad (1)$$

The room temperature mechanical strength of the sintered specimens was determined by three-point flexural tests. The specimens were machined into test bars shape with a dimension of $3 \times 4 \times 25$ mm^3, and all the surfaces of the bars were ground with a 600-grit diamond wheel and edges were beveled. The direction of both the diamond grinding and the beveling was parallel to the bar length. Three-point bending strength was measured on bars using a span of 16 mm and a crosshead speed of 0.5 mm/min (Instron 1195; Instron, UK). By repeating the tests for silicon nitride three times for each specimen, the results are given as the mean values of three measurements.

Phase analysis was conducted by X-ray diffraction (XRD), via a computer controlled diffractometer (XRD-6000; Shimadzu). Fracture surfaces of the sintered bodies were observed using scanning electron microscopy (SEM; S-270; Hitachi) to estimate the microstructure uniformity of the specimens. Pore-size distributions of the sintered bodies were measured using high-pressure porosimeter (Autoscan 33, Quantachrome Corp., USA).

The complex permittivity of porous Si_3N_4 was measured at 8–18 GHz by a resonant cavity method at room temperature, and the dimensions of the test specimens were approximately 54 mm in diameter and 2.3 mm in thickness. The instrument used to determine the complex permittivity was manufactured by the National Key Laboratory of Advanced Functional Composites Materials, Beijing, China.

Results and discussion

Porosity and linear shrinkage

The porosity of porous Si_3N_4 ceramics is controlled only by low molding pressure (10 MPa) and pressureless-sintering without the pore forming agent, and thus the purity of the porous Si_3N_4 ceramics is high. Table 1 shows

Table 1 Summary of density, porosity, and shrinkage of the sintered porous Si_3N_4 ceramics

Sintering temperature(°C)	Holding time (min)	Shrinkage (%)	Density (g/cm^3)	Porosity (%)		
				Total	Open	Closed
1630	60	2.00	1.29	59.5	59.2	0.3
	120	3.86	1.44	54.9	54.5	0.4
1680	60	3.20	1.41	55.7	55.3	0.4
	120	5.16	1.52	52.4	51.9	0.5
1730	60	4.72	1.57	50.8	50.4	0.4
	120	11.26	1.92	39.8	39.4	0.4
1780	30	5.37	1.63	49.4	49.0	0.4
	60	6.03	1.61	45.8	45.7	0.1
	120	12.7	2.03	36.3	35.7	0.6

the influences of sintering temperature on the shrinkage, density, and porosity of sintered porous Si_3N_4 ceramics.

The results show that the total porosity decreases from 59.5 to 45.8%, the linear shrinkage increases from 2 to 6%, and the density increases from 1.29 to 1.61 g/cm^3 with the sintering temperature increasing from 1630 to 1780 °C holding for 60 min. The sintering of Si_3N_4-based ceramics is a complex densification process, and phase transformation and grain growth take place simultaneously [20]. The densification of Si_3N_4 ceramics using Y_2O_3–Al_2O_3 system as sintering aids begins at temperature above 1400 °C [21], at which the glass phase formed and particle rearrangement are the main densification mechanism [22]. And the viscosity of glass phase (sintering aids) is the main factor to influence the densification process. In this experiment, the total content of sintering aids (Y_2O_3 and Al_2O_3) is only 8 wt%, which is lower than that of previous work [23]. The low content of the glass phase (sintering aids), the low viscosity of the glass phase (sintering aids), and pressureless sintering lead to a low linear shrinkage (2–6%) and a little increase of the density (1.29–1.61) with the sintering temperature increasing from 1630 to 1780 °C. Low linear shrinkage indicates that original pores (due to low molding pressure (10 MPa)) in the powder compact remain after sintering, and thus the porous Si_3N_4 ceramics with porosity (45.8–59.5%) are obtained.

X-ray diffraction and microstructure

The XRD patterns of samples sintered at 1680, 1730, and 1780 °C for 60 min are shown in Fig. 1. The content of sintering aids is low, and thus there is no other phase in XRD patterns except for α or β-Si_3N_4 phase.

The α–β transformation at temperature of 1680 °C is incomplete, and a large amount of α-Si_3N_4 remains in the sample. The formation of β-Si_3N_4 is enhanced when heating up to higher temperature, heating to 1730 and 1780 °C directly results in the formation of β-Si_3N_4 single phase, as shown in Fig. 1.

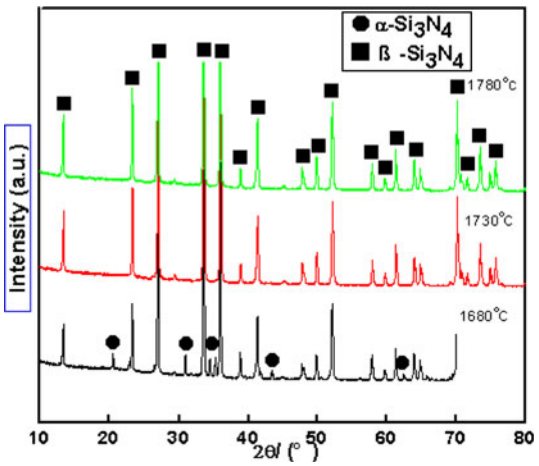

Fig. 1 XRD patterns of the samples sintered at different temperature holding for 60 min

Figure 2 shows the microstructures of samples sintered at 1680, 1730, and 1780 °C for 60 min. The microstructures are uniform, and the β-Si_3N_4 can be easily identified in SEM micrograph due to its elongated grains. The β-Si_3N_4 is a high temperature phase and can be formed through dissolution of α-Si_3N_4 particles and precipitation as β-phase in a liquid phase. The α–β phase transformation occurs at 1680 °C (Fig. 2a), where large amount of equiaxial α-Si_3N_4 and less developed fibrous β-Si_3N_4 is detected. With the increase of the sintering temperature, it can be seen that the well-developed fibrous β-Si_3N_4 microstructure is achieved at 1730 and 1780 °C (Fig. 2b, c), this microstructure feature can be obtained by α–β phase transformation in sintering through a solution–precipitation process [24], and these β-Si_3N_4 are overlapped each other, which makes the samples have higher flexural strength.

Figure 3 shows the influences of sintering temperature on the pore size distribution of porous Si_3N_4 with the same holding time (60 min). It is observed that the pore size is uniform and less than 1 μm, and the samples sintered at lower temperature show a finer pore size distribution.

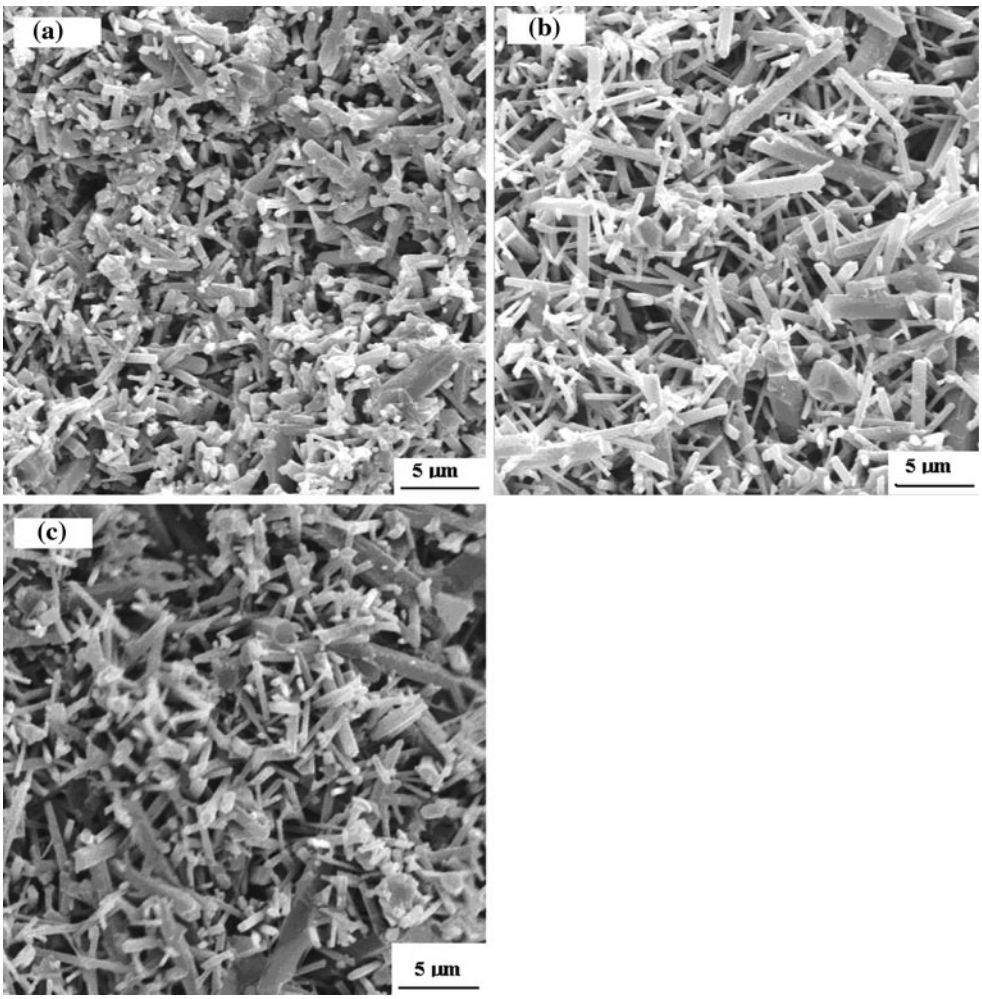

Fig. 2 SEM micrographs of porous Si_3N_4 sintered at **a** 1680 °C, **b** 1730 °C, and **c** 1780 °C holding for 60 min

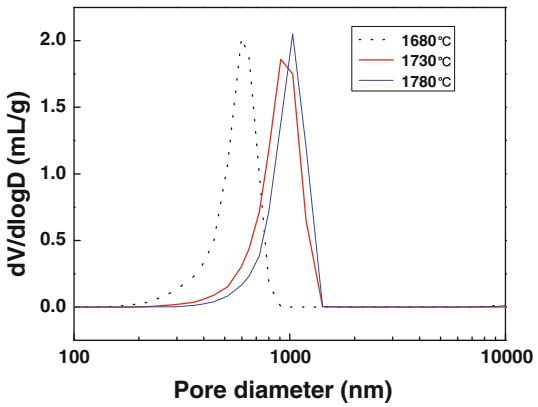

Fig. 3 Pore size distributions of porous Si_3N_4 at different sintering temperatures holding for 60 min

Flexural strength

Figure 4 shows the influences of sintering temperature on flexural strength of porous Si_3N_4 ceramics with the same holding time (60 min). The results showed that the flexural strength of samples increase from 57 to 176 MPa when the sintering temperature varies from 1630 to 1780 °C. The flexural strength variation trends of porous Si_3N_4 ceramics and density with the sintering temperature are similar, and high flexural strength can be achieved by high density. For Si_3N_4-based ceramics, the fibrous-Si_3N_4 grains overlapped each other could be beneficial for the mechanical properties of the resultant specimens. Using α-Si_3N_4 as precursor powder, X-ray diffraction and SEM structural analyses reveal complete phase transformation and fine fibrous β-Si_3N_4 grains formation by heating the appropriate powder compacts at above 1730 °C (1730 and 1780 °C). Porous Si_3N_4 ceramics with a microstructure of interconnected fibrous β-Si_3N_4 grains bonded together have better mechanical properties.

The flexural strength of porous ceramics is very strongly dependent on the porosity. The dependence of flexural strength on porosity has been extensively investigated, and their relationship can be expressed by the following expression [25, 26]:

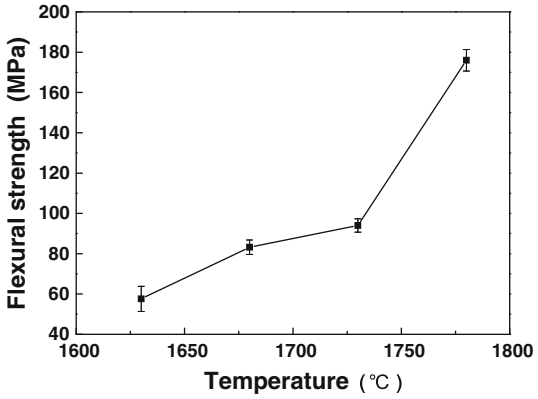

Fig. 4 The influences of sintering temperature on flexural strength of porous Si_3N_4 ceramics (60 min)

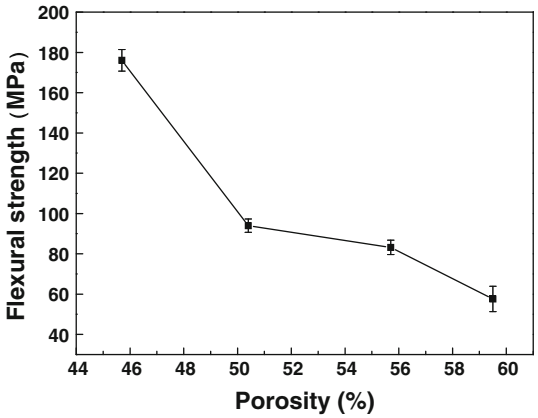

Fig. 5 The relationship between flexural strength and porosity

$$\sigma_f = \sigma_0 e^{(-np)} \quad (2)$$

where σ_0 is the strength at a porosity of 0, n is the structural factor, and P is the porosity.

Figure 5 shows the relationship between the flexural strength and the porosity of porous Si_3N_4 ceramics. The flexural strength is obviously affected by the porosity, and the flexural strength significantly decreases with the increase of porosity. The porosity increases from 45.7 to 59.5% with the flexural strength decreasing from 175 to 57.6 MPa.

In this article, the formation of pores is relative to low molding pressure (10 MPa), pressureless sintering and the formation of a three dimensional network structure by fibrous β-Si_3N_4 grains.

Dielectric properties

Figure 6 shows the influences of the frequency on the dielectric constant and dielectric loss of porous Si_3N_4 ceramics sintered at 1730 °C for 60 min. It shows that the

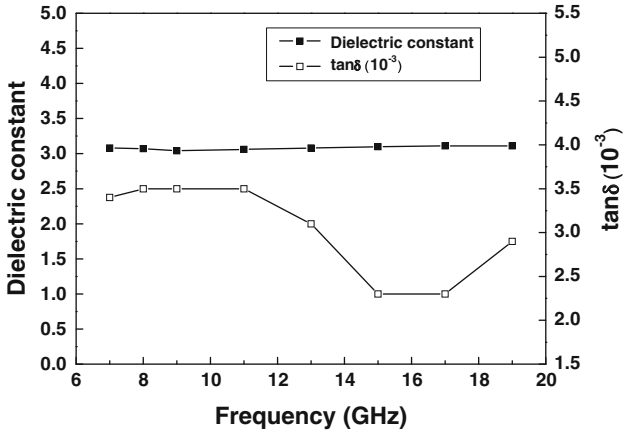

Fig. 6 The influences of the frequency on the dielectric constant and dielectric loss (tanδ) of porous Si_3N_4 ceramics (1730 °C, 60 min)

dielectric constant has minor variation with the change of the frequency (8–18 GHz), the dielectric constant varies from 3.04 to 3.11, the dielectric loss varies from 2.3–3.5 $\times$ 10^{-3}. Above the frequency of 13 GHz, the tanδ decreases first and then increases with the increase of the frequency, which may be caused by the water vapor in the pores, similar with reference [27]. According to the dielectric theory, at the low frequency, the influence of the polarization of water is ignorable, but with the frequency increasing, the contribution of the water to the dielectric loss becomes more and more important, which makes the dielectric loss decrease.

Figure 7 shows the influences of porosity on the dielectric constant (ε) and tanδ of the porous Si_3N_4. With the increase of porosity, the ε and tanδ of the porous Si_3N_4 monotonically decrease.

According to the mixture rule, the dielectric constant of the well-distributed two-phase composite is calculated as follow [28]:

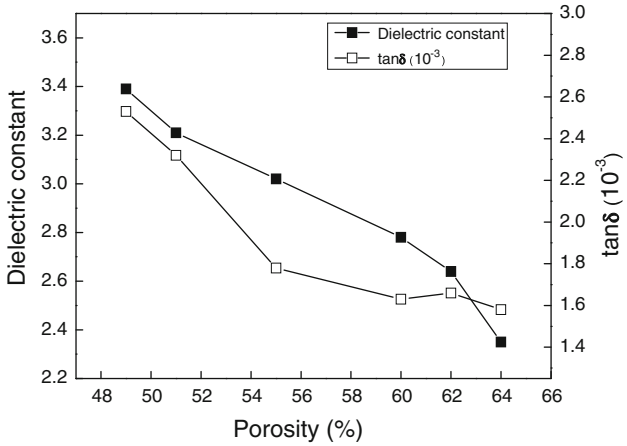

Fig. 7 The influences of the porosity on the dielectric constant (ε) and dielectric loss (tanδ) of the porous Si_3N_4 ceramics

$$\varepsilon = V_1\varepsilon_1 + V_2\varepsilon_2 \quad (3)$$

where ε is the dielectric constant of the composite, V_1 and V_2 are the volume fractions of phase 1 and phase 2, ε_1 and ε_2 are the dielectric constant of the two phase, respectively. As porous Si_3N_4 ceramics, pores are the main phases which influence the composite's dielectric properties. As we all know, the dielectric constant of air is 1 and the dielectric loss is approximately equal to 0, and thus the Eq. 3 can be expressed as follow:

$$\varepsilon = \varepsilon_0 - P(\varepsilon_0 - 1) \quad (4)$$

where ε_0 is the theoretical dielectric constant of main phase, and P is the porosity [29]. Equation 4 shows that the dielectric constant of porous ceramic decreases with the increase of porosity, which is consistent with the results of Fig. 7.

Conclusions

(1) Porous Si_3N_4 ceramics with high flexural strength are obtained by low molding pressure (10 MPa) and pressureless sintering process without any other pore forming agents.
(2) Porous Si_3N_4 ceramics not only have high mechanical properties but also have low dielectric constant. The flexural strength of porous Si_3N_4 ceramics varies from 57 to 176 MPa, the porosity varies from 45 to 60%, the dielectric constant varies from 2.35 to 3.39, and the dielectric loss varies from 1.6–3.5 $\times$ 10^{-3} in the frequency range of 8–18 GHz, at room temperature.
(3) Flexural strength, dielectric constant, and dielectric loss all decrease with the increase of porosity.

Acknowledgements This work was supported by the National Natural Science Foundation of China (90816018), the project of National Laboratory of Advanced Functional Composite Materials (9140C5602040805), and Xi'an Science and Technology Program (CXY08006(1)).

References

1. Koetje EL, Simpson FH (1987) US Patent 4677443
2. Jain V, Varshneya AK, Bihuniak PP (1990) J Am Ceram Soc 73:409
3. Kicevic D, Gasic M, Markovic D (1996) J Eur Ceram Soc 16:857
4. Kawai C, Matsuura T, Yamakawa A (1999) J Mater Sci 34:893. doi:10.1023/A:1004532200735
5. Yang JF, Ohji T, Kanzaki S (2002) J Am Ceram Soc 85:1512
6. Ding SQ, Zeng YP, Jiang DL (2007) Mater Lett 61:2277
7. Walton JD (1974) Am Ceram Soc Bull 53:255
8. Barta J, Manela M, Ficher R (1985) Mater Sci Eng 71:265
9. Gota T, Fujii A, Kawai C (2000) US Patent 6091375
10. Kawai C, Yamakawa A (2002) J Am Ceram Soc 80:2705
11. Lyckfeldt O, Ferreira JMF (1998) J Eur Ceram Soc 18:131
12. Fu XP, Qiu FG, Liu XJ (2005) J Inorg Mater 20:1431
13. Ramay HR, Zhang MQ (2003) Biomaterials 24:3293
14. Fukasawa T, Deng ZY, Ando M (2002) J Am Ceram Soc 85:2151
15. Zhang Y, Wang HJ, Jin ZH (2004) Rare Metal Mat Eng 33:655
16. Zhang W, Wang HJ, Jin ZH (2005) J Mater Sci Technol 21:894
17. Zhang W, Wang HJ, Jin ZH (2005) Mater Lett 59:250
18. Yu JL, Wang HJ, Zeng H (2009) Ceram Int 35:1039
19. Xia YF, Zeng YP, Jiang DL (2009) Ceram Int 35:1699
20. Li XM, Yin XW, Zhang LT et al (2009) Mater Sci Eng A 500:63
21. Yang JF, Ohji T, Konda N (2000) J Am Ceram Soc 83:2094
22. Yang JF, Zhang GJ, Konda N (2002) Acta Mater 50:4831
23. Wang HJ, Wang YL, Jin ZH (1997) J Mater Sci 32:5775. doi:10.1023/A:1018678019734
24. Shen ZJ, Zhao Z, Peng H, Nygren M (2002) Nature 417:266
25. Coble RL, Kingery WD (1956) J Am Ceram Soc 39:377
26. Ryshkewitch E (1953) J Am Ceram Soc 36:65
27. Zhang L, Jin H, Cao M (2007) Rare Metal Mater Eng 36:515
28. Kingery WD, Bowen HK, Uhlmann DR (1976) Introduction of ceramics. Wiley, USA
29. Penn SJ, Alford NM, Templeton A (1997) J Am Ceram Soc 80:1885